

Isotopic fractionation of Zn in tektites

Frederic Moynier^{1,2,*}, Pierre Beck³, Fred Jourdan⁴, Qing-zhu Yin², Christian Koeberl⁵, and Uwe Reimold⁶

¹Department of Earth and Planetary Sciences, Washington University in St Louis, One Brookings Drive, St Louis, MO 63130

²Department of Geology, University of California Davis. One Shields Avenue, Davis, CA 95616

³Laboratoire de Planetologie, Universite Joseph Fourier, CNRS/INSU, Bat. Physique D, BP 53, 38041 Grenoble cedex 9, France

⁴ Western Australian Argon Isotope Facility, Department of Applied Geology & JdL-CMS, Curtin university of Technology, GPO Box U1987, Perth, WA 6845; Australia.

⁵Department of Lithospheric Research, University of Vienna, Althanstrasse 14, A-1090 Vienna, Austria

⁶Museum f. Natural History (Mineralogy), Humboldt University Berlin, Invalidenstrasse 43, 10115 Berlin, Germany

*Corresponding author: moynier@levee.wustl.edu, Tel: +1 314-935-8634, Fax: +1 314-935-7361

Abstract: Tektites are terrestrial natural glasses, produced during a hypervelocity impact of an asteroid (or comet nucleus) into the Earth surface. The similarity between the chemical and isotopic compositions of tektites and terrestrial upper continental crust implies they formed from the target rocks. The mechanism of the loss of water as well as the behavior of volatile species during tektites formation is still debated, and volatilization at high temperature is a possible way. Volatilization can fractionate isotopes, and, therefore, comparing the isotope composition of volatile elements in tektites with their source rocks may help to understand the conditions of evaporation.

In this study, we have measured the Zn isotopic composition of 20 tektites from the four different strewn fields. Almost all the samples are enriched in heavy isotopes of Zn compared to the upper continental crust. On average the different groups of tektites are isotopically distinct and give the following values (from the isotopically lightest to the heaviest): Muong-Nong type indochinites ($\delta^{66/64}\text{Zn}=0.61\pm 0.30\text{‰}$; 1σ); the North American bediasites ($\delta^{66/64}\text{Zn}=1.61\pm 0.49\text{‰}$); the Ivory Coast tektites ($\delta^{66/64}\text{Zn}=1.66\pm 0.18\text{‰}$); the Australasian tektites (others than the Muong Nong-type indochinites) ($\delta^{66/64}\text{Zn}=1.84\pm 0.42\text{‰}$) and the Central European moldavites ($\delta^{66/64}\text{Zn}=2.04\pm 0.19\text{‰}$).

$\delta^{66/64}\text{Zn}$ is negatively correlated with the abundance of Zn, which may reflect that the isotopic fractionation occurred by evaporation during the heating event of the tektites. Simple Rayleigh distillation predicts isotopic fractionations much larger than what is actually observation, and, therefore, such a model cannot account for the mechanism of fractionation of Zn isotopes in

tektites. We developed a more realistic model of evaporation of Zn from a molten sphere: during its hypervelocity trajectory, the molten surface of the tektite will be entrained by viscous coupling with air, which will then induce a velocity field inside the molten sphere. This velocity field induces significant radial chemical mixing within the tektite which fastens the evaporation process. Our model, even if parameter dependent, shows that both the isotopic composition and the chemical abundances measured in tektites can be produced by evaporation in a diffusion-limited regime.

1. Introduction:

Tektites are terrestrial natural glasses, produced during the early phases of a hypervelocity impact of an asteroid (or comet nucleus) into target terrestrial rock (e.g., Blum et al., 1992; Glass, 1990; Koeberl, 1986; 1990; 1992, 1994). The chemical and isotopic compositions of the tektites are similar to that of the terrestrial upper continental crust (see reviews in Koeberl, 1986, 1994) and, therefore, tektites formed from the target rocks and not from the projectile. In addition, studies of cosmogenic radioisotopes (e.g., ^{10}Be) have shown that tektites must have been derived from the very top of the impacted target (see Ma et al., 2004; Serefiddin et al., 2007, and review in Koeberl, 2007). However, osmium isotope studies have shown that a very small, but measurable extraterrestrial signature is also present in at least some tektites (Koeberl and Shirey, 1993).

As expected from their impact origin, tektites are only found in a few distinct geographical areas, the so-called strewn fields, of which four are currently known: the North American (~35 Ma); Central European (~14.4 Ma), Ivory Coast (~1.07 Ma), and Australasian (~0.8 Ma) strewn fields. The tektites from these four different strewn fields are characterized by different chemical compositions, petrological properties, and ages. In addition to their different geographical origin the tektites found on land (to be opposed to the microtektites found in the deep-sea cores) are classified into three groups: (i) aerodynamically shaped tektites; (ii) normal or splash-form tektites (iii) Muong Nong (or layered) tektites. (i) and (iii) are predominantly found in the Australasian strewn fields. The aerodynamic ablation results from partial re-melting of the tektite glass during atmospheric re-entry after it was ejected outside the terrestrial atmosphere and solidified through quenching. Such aerodynamically shaped tektites are known mainly from the Australasian strewn field, primarily as flanged-button australites. The shapes of splash-form tektites are not aerodynamical forms, but result mostly from the solidification of rotating liquids. Muong Nong tektites are usually considerably larger than normal tektites and are of chunky, blocky appearance.

The source craters for three of the four strewn fields have been identified: the Chesapeake Bay crater (USA) for the North American strewn field; the Bosumtwi crater (Ghana) for the Ivory Coast strewn fields and the Ries Crater for the Central European strewn field (see Koeberl, 1994, for a summary). The crater at the origin of the Australasian strewn field has not yet been found.

Tektites are water-poor glasses (<0.02 wt%) in comparison to their possible precursor terrestrial rocks (typically sedimentary rocks have >1 wt% of water). Vapor fractionation at very high temperature (>2800 °C for 5-10 minutes or >3000 °C for less than a minute) and under oxidized conditions (Walter, 1967) has been proposed as a possible origin for the water loss. However, this model has some flaws (e.g. how to keep the low $\text{Fe}^{3+}/\text{Fe}^{2+}$ ratio, as it is observed in tektites, under these conditions of temperature and oxidation state) and therefore the behavior of volatile elements and molecules during tektites formation is still debated.

Volatilization is known to fractionate isotopes, and, therefore, comparing the isotope composition of volatile elements in tektites with their source rock may help to understand the conditions of evaporation. Variability in the isotope composition of the source rocks is usually a problem for many “light” elements (H, O...), which are fractionated by several mechanisms other than evaporation. Though, this variation in the isotopic composition of the source rocks of light elements can be used to trace the origin of the tektites. For example, Chaussidon and Koeberl (1995) analyzed the B isotope composition of tektites from different strewn fields. They found that Australasian tektites have the B isotope composition of pelagic and neritic sediments

whereas Bediasitic tektites have the same B isotope composition as marine carbonites or evaporites. Most tektites show no or small isotopic enrichments in ^{18}O in comparison to the average composition of granites and are almost indistinguishable from terrestrial soil (Taylor and Epstein, 1962). However, bediasites are an exception because their O isotopic composition is negatively correlated with the content of silica of the tektites (Taylor and Epstein, 1964). Walter and Clayton (1967) performed high temperature experiments and proved that evaporation is a mechanism suitable for both the origin of the O isotopic fractionation and the decrease in the content of SiO_2 in bediasites. Therefore, “heavy stable” isotopes, which show no or little variability in terrestrial upper crustal rocks, are more suitable targets for such a study. Following this rationale, Humayun and Koeberl (2004) measured the K isotope composition in four tektites from the Australasian strewn field and did not find any variations between the tektites and the terrestrial rocks. The absence of K isotope fractionation is a surprise because it is a moderately volatile element with a 50% condensation temperature (T_c) of $\sim 1000\text{K}$ (Lodders, 2003), and K isotopes are fractionated strongly in lunar regolith (Humayun and Clayton, 1995). Based on the absence of K isotopic fractionation in tektites, Humayun and Koeberl (2004) placed an upper limit of loss of K at $<2\%$ and concluded that any other less volatile elements should not be fractionated during the heating events experienced by tektites. More recently, Herzog et al. (2005) observed that micro-tektites are isotopically fractionated in K, some micro-tektites being enriched in light isotopes (up to $-10.2 \pm 0.5 \text{‰}$) and other in heavy isotopes (up to $14.1 \pm 0.5 \text{‰}$); however, on average the micro-tektites were isotopically normal ($1.1 \pm 1.7 \text{‰}$). This implies that, in contrast to tektites, micro-tektites experienced both evaporative loss of isotopically light K and re-condensation of isotopically heavy K.

Here we apply the same logic to Zn. Zinc is a moderately volatile element, more volatile than K, with $T_c(\text{Zn}) \sim 730\text{K}$ (Lodders, 2003) and Zn has a very limited isotopic variation in terrestrial rocks. In addition, it has been recently shown that isotope fractionation of Zn in lunar soils (Moynier et al., 2006) is very large (up to 3‰ per amu). These fractionations have been attributed to vaporization due to impact by micrometeorites onto the surface of the moon. In addition, recently Albarede et al. (2007) extended the study of isotopic fractionation of Zn to shocked rocks from a terrestrial impact site, Meteor Crater. They observed a negative correlation between isotope compositions and shock grade in seven samples of Coconino sandstone and concluded that, on Earth, vaporization at high temperature due to impact is capable of fractionating the isotopic compositions of rather heavy elements to a measurable extent.

Because it is a moderately volatile element that shows no or little fractionation in terrestrial rocks, and for which large isotopic fractionations have been found in lunar soils and in shocked rocks from terrestrial impact craters, Zn is a very suitable element to search for isotopic fractionation due to volatile processes in tektites.

Here, we investigate the degree of isotopic fractionation of Zn in 20 different tektites from the four different strewn fields, as well as in the impact melt rocks from the Bosumtwi crater (Ghana). The Zn isotopic composition of a non-tektite impact glass, a Libyan Desert Glass (LDG), has also been measured for comparison. We also report the chemical composition of major and trace elements of the samples for which these data were unavailable.

2. Samples and analytical methods:

2.1. Sample description:

We analyzed the following samples:

1) Three Ivory Coast (IVC) tektites: IVC-2014, IVC-3395, and IVC-8902. The ~1.07 Ma (Koeberl et al., 1997) Bosumtwi impact crater in Ghana is recognized as the source for the IVC, based on similar geochemistry and ages of tektites and crater-based impact melt (e.g., Koeberl et al., 1997, 1998). Our samples (IVC-2014, IVC-3395, IVC-8902) have already been analyzed for their major and trace element composition by Koeberl et al. (1997). For comparison we also analyzed the Zn isotopic composition of two impact melt clasts from suevite samples from the Bosumtwi crater, Ghana (samples 2004/3 and LB-43). Different target rocks exist at the Bosumtwi crater and so these two suevites are not fully representative of the Bosumtwi crater, however, for now we consider these samples as our best estimate for the target rocks of the IVC tektites. Details for sample LB-43 are described in Karikari et al. (2007).

2) Nine Australasian tektites: Six Muong Nong-type tektites (MN 8301, MN 8309, MN 8314, MN X102, MN X103 and Hainan HFS1); two Australites (5772 and T8205), with the australite 5772 being a typical flanged-button australite, for which we separately analyzed the rim and the core for Zn isotopic compositions and chemical composition, whereas T8205 was only analyzed in bulk; two philippinites (1995 and 9201) and one thailandite (8204). MN 8301, 8309, 8314, X102 and X103 have already been analyzed for their major and trace elements composition in Koeberl (1992). For all other samples, the major and trace element compositions were measured in this study. The impact crater at the origin of the Australasian tektites is not yet known.

3) Four Central European tektites: one moldavite from Clum (MC), and three moldavites from Jankov (Jankov 1, 2, and 4). These four samples were not been analyzed for anything else and therefore we measured both Zn isotopic composition and bulk elemental composition. The Ries crater (Germany) has been determined as the source of the central European tektites (e.g., Engelhardt et al., 1987).

4) Two North American tektites: Bediasite (BED8401 and BED8402). These two bediasites have been described in Weinke and Koeberl (1985). The Chesapeake impact crater in USA has been recognized as the source for the North American tektites (Koeberl et al., 1996).

In addition, we analyzed the Zn isotope composition and the major and trace element composition of a Libyan Desert Glass, LDG 8501. This glass has already been described in Koeberl (1985).

2.2 Analytical methods:

Fragments of tektites or powders of ~150 mg were cleaned in water for 5 minutes in an ultrasonic bath, the leaching solution was removed and then the residue was dissolved in HNO₃/HF at 130°C for several days in closed Teflon beakers.

Zinc was purified by anion-exchange chromatography using a procedure described in Moynier et al. (2006; 2007). Briefly, samples were loaded in 1.5N HBr on 0.25 ml AG-1X8 (200-400 mesh) chromatographic columns and Zn was extracted in 0.5N HNO₃. The process was repeated on a 100 µl column to further purify Zn. Zinc isotopic compositions were measured on a Nu Plasma High Resolution Multi Collection-Inductively Coupled Plasma-Mass Spectrometer (MC-ICP-MS) at the University of California, Davis, as described in Moynier et al. (2006). The yield was checked and found to be better than 99% and the blank of ~10 ng is negligible with respect to the total amount of Zn in the samples, which is >2 µg. Isotope ratios are expressed as relative deviations, δ , given by the standard relations

$$\delta^x\text{Zn} (\text{‰}) = \left(\frac{\left(\frac{{}^x\text{Zn}}{{}^{64}\text{Zn}} \right)_{\text{sample}}}{\left(\frac{{}^x\text{Zn}}{{}^{64}\text{Zn}} \right)_{\text{standard}}} - 1 \right) \times 1000 \quad (1)$$

with $x = 66$ or 68 . The reference is the Zn “Lyon” standard JMC 3-0749 L (Marechal et al. 1999). In replicate analyses of the same samples carried out during different sessions, we obtained an external reproducibility of $\pm 0.09\text{‰}$ for $\delta^{66}\text{Zn}$ and $\pm 0.27\text{‰}$ for $\delta^{68}\text{Zn}$ (see Moynier et al. 2006; 2007; in press)

The chemical abundances have been measured at ENS Lyon, France by ICP-MS (Agilent 7500CX) for the trace elements and by inductively coupled plasma atomic emission spectroscopy (ICP-AES, iCAP Thermo), for the major elements. For the chemical abundance measurements, samples of 100-200 mg were dissolved in the same conditions as described above for the isotopic composition measurements. After dissolution each sample has been re-dissolved in dilute nitric acid and doped with a standard of indium to correct for instrument derivation with time. International standard reference materials used were.... Error on the major and trace elements varie between $\pm xx\%$ and $\pm xx\%$ and $\pm xx\%$ and $\pm xx\%$ respectively, depending on the concentration of the element.

3. Results:

Isotope ratios are reported in the Table 1 in δ permil units with respect to the standard JMC 0749 L. As expected from mass-dependent isotopic fractionation, all the samples (but one) plot onto a straight line of slope 2 in a $\delta^{68/64}\text{Zn}$ vs $\delta^{66/64}\text{Zn}$ diagram (Fig. 1). The sample plotting outside the mass-fractionation line is the core of the australite tektite 5572 and this is probably due to some unidentified interferences on the MC-ICP-MS. It implies that this data is not as precise as the other ones, and we will not give much weight to this data in the rest of the paper. The full range in $\delta^{66/64}\text{Zn}$ is about 2 permil. The isotopically heaviest sample is the philippinite 1995 ($\delta^{66/64}\text{Zn} = 2.49 \pm xx \text{‰}$) and the isotopically lightest sample is the Muong Nong-type tektite MN8301 ($\delta^{66/64}\text{Zn} = 0.31 \pm xx \text{‰}$). On average the different groups of tektites are isotopically distinct and give the following values (from the isotopically lightest to the heaviest): Muong-Nong type indochinites ($\delta^{66/64}\text{Zn} = 0.61 \pm 0.30 \text{‰}$; 1σ); the North American bediasites ($\delta^{66/64}\text{Zn} = 1.61 \pm 0.49$); the Ivory Coast tektites ($\delta^{66/64}\text{Zn} = 1.66 \pm 0.18 \text{‰}$); the Australasian tektites (others than the Muong Nong-type indochinites) ($\delta^{66/64}\text{Zn} = 1.84 \pm 0.42 \text{‰}$) and the Central European moldavites ($\delta^{66/64}\text{Zn} = 2.04 \pm 0.19 \text{‰}$).

The rim ($\delta^{66/64}\text{Zn} = 1.83$) of the flanged australite 5572 is slightly isotopically heavier than the core ($\delta^{66/64}\text{Zn} = 1.22$). Australites are supposed to be formed in two steps: first the high velocity impact of an asteroid with the target rock produced a melt-droplet (the future core of the australite), which is travels above the Earth’s atmosphere; second, during its re-entry in the atmosphere the core is heated and re-melted at its surface. The re-melted surface forms the rim (Taylor, 1961).

Despite coming from different target rocks, the Libyan Desert Glass 8501 has a $\delta^{66/64}\text{Zn}$ of 0.61, which is comparable with the mean value of the Muong Nong-type tektites, and fall in the typical terrestrial range (0-0.7‰, see below)

The two melt rock samples from the Bosumtwi crater have normal terrestrial isotopic compositions in Zn ($\delta^{66/64}\text{Zn} = +0.17$ and $+0.46$) and so we can infer that the IVC tektites have been fractionated from their source by more than 1 ‰.

The chemical abundances are given in Table 2. Our results acquired by ICP-MS and ICP-AES for the LDG8501 and bediasites 8401 and 8402 agree well with previous published data from Koeberl (1985) and Weinke and Koeberl (1985) acquired with a different technique (neutron activation and electron microprobe).

4. Discussion

4. 1. The rocks with the heaviest Zn isotopic composition on Earth?

Zinc isotopes have a very homogeneous composition in terrestrial rocks, with a typical isotopic composition in $\delta^{66/64}\text{Zn}$ between 0 and 0.60 ‰ in igneous rocks (Ben Othman et al., 2006; Cloquet et al., 2006; Marechal, 1999) and up to 0.70 ‰ in some sedimentary rocks and ores (Albarede, 2004; Pichat et al. 2003). In contrast, all of the tektites measured in this study (with exception of the Muong Nong-type tektites, and also the Libyan Desert Glass) are greatly enriched in the heavy isotopes ($+1.22 < \delta^{66/64}\text{Zn} < +2.49$) and are, to our knowledge, the isotopically most Zn-fractionated terrestrial samples analyzed to date. Philippinite 1995 is the terrestrial sample ($\delta^{66/64}\text{Zn} = +2.49 \pm \text{xx}$) with the heaviest Zn isotopic composition. Other than tektites, other terrestrial materials that show heavy Zn isotope compositions, are manganese nodules from the circum-artic with a $\delta^{66/64}\text{Zn}$ of ~ 1.16 ‰ (Maréchal et al., 2000). This isotopic fractionation in Mn nodules has been suggested to reflect preferential uptake of light isotopes by the biological activity in the upper water column leading to the water (presumably equilibrated with the Mn nodules) being enriched in the heavy isotopes of Zn. Natural samples with isotopically light Zn (negative $\delta^{66/64}\text{Zn}$, up to $-x.xx$ ‰) are not very common and the largest effects seem to be almost limited to biological material (John et al. 2007; Moynier et al. in press; Viers et al. 2007; Weiss et al., 2005), reflecting the preferential uptake of light isotopes by biological activity.

In the solar system, the only natural samples known so far to be heavier in Zn than tektites are lunar regoliths with $\delta^{66/64}\text{Zn}$ up to $+6.39$ ‰ (Moynier et al., 2006).

Because the exact Zn isotope compositions of the target rocks and of the meteorites are not known, an origin of the isotopic fractionation by mixing or by secondary alteration can not be totally excluded. However, the isotopic variation of Zn in normal crustal rocks known so far is limited between 0.00 and 0.70 ‰ (Albarede, 2004; Ben Othman et al., 2006), and thus it would be very unlikely that the isotopic fractionation observed in tektites (up to 2.49 ‰) is related to alteration. Therefore, the enrichment in heavy isotopes of Zn in tektites can be more likely explained by the loss of isotopically light Zn that was concentrated in the vapor fraction during the heating events experienced by tektites.

The Muong Nong-type tektites are known to be less depleted in volatile elements than splash-form tektites (e.g., Koeberl, 1992, 1994). They are also the ones that remain closest to the site of the impact (e.g., Koeberl, 1994; Ma et al., 2004). As expected from vapor fractionation, the Muong Nong-type tektites have the lowest Zn isotopic fractionation among all the tektites analyzed here. They do show, as the other tektites, a clear, but less pronounced enrichment in the heavy Zn isotopes.

4. 2. Origin of the Zn isotopic fractionation

The stable isotopes of light elements, notably Mg (Esat and Taylor, 1986, 1987), B (Chaussidon and Koeberl, 1995), and K (Humayun and Koeberl, 2004) have already been measured in tektites without any clear indication for isotopic fractionation with respect to terrestrial rocks. O isotopes do not show any isotopic variations in most of all the tektites in comparison to the average composition of granites and it is hardly impossible to differentiate them from the terrestrial soil (Taylor and Epstein, 1962). The same authors further measured in bediasites slight isotopic enrichments in ^{18}O negatively correlated with their SiO_2 content (Taylor and Epstein, 1964). Walter and Clayton (1967) further shown experimentally that high temperature evaporation can be at the origin of both the O isotopic fractionation and the decrease in the content of SiO_2 . Magnesium is a fairly refractory element and does not show any fractionation in lunar regolith. It is thus not surprising that this element does not show fractionation in tektites. The absence of K isotope fractionation is a surprise because it is a moderately volatile element with a 50% condensation temperature (T_c) of ~ 1000 K (Lodders, 2003), and K isotopes are fractionated strongly in lunar regolith (Humayun and Clayton, 1995). Based on the absence of K isotopic fractionation in tektites, Humayun and Koeberl (2004) placed an upper limit of loss of K at $<2\%$ and concluded that any other less volatile elements should not be fractionated during the heating events experienced by tektites. However, microtektites show large K isotopic fractionations (Herzog et al. 2005) and, therefore, it seems that K isotopes can be fractionated at the surface of the tektites. Also B is a moderately volatile element ($T_c \sim 800\text{K}$; Lodders, 2003) and does not seem to show any fractionation in tektites (Chaussidon and Koeberl, 1995). Zinc is a more volatile element than both B and K ($T_c \sim 730\text{K}$ (Lodders, 2003)) and the isotopic fractionation of Zn measured in this study may reflect the loss of Zn during the heating of the tektites. This conclusion is supported by the strong depletion of Zn in tektites compared to target rocks, more than many other similarly volatile elements (Greenland et al. 1962; Koeberl et al. 1986, 1992). This depletion in Zn is confirmed by our measurements and are in fairly good agreement with the average Zn content measured in the different tektite groups by Greenland et al. (1963): for the thailandite (7.6 ppm), the moldavites (20 - 28 ppm), the bediasites (10.9-26ppm), and the philipinites (18.6 - 23.1 ppm). For the australites our data (16.4 ppm) is within the range (3.2-19 ppm) measured by Greenland et al. (1962) in 21 australites but, surprisingly, is almost 10 times higher than what has been reported previously by Koeberl (1986) (~ 2 ppm). Nevertheless, Zn is depleted in all the tektites with regards to the terrestrial upper crust ($\sim 67 \pm 6\text{ppm}$; cf. Rudnick and Gao, 2003).

Figure 2 shows a negative correlation between $\delta^{66/64}\text{Zn}$ vs $[\text{Zn}]$ for all the bulk tektites analyzed here at the exception of the IVC2014 and IVC3395 which have surprisingly low Zn content. As expected if the origin of the isotopic fractionation is evaporation, the isotopic composition is getting heavier when the Zn content decreases. This correlation is even more pronounced when only tektites from the same group are plotted. Figure 3 is an example of a $\delta^{66/64}\text{Zn}$ vs $[\text{Zn}]$ plot for the Australasian tektites (this is the group for which we have the largest number of samples). Assuming that evaporation obeys a simple Rayleigh distillation law (Eq. 2), the evolution of the expected $\delta^{66/64}\text{Zn}$ in function of the remaining fraction of Zn is plotted in the Fig. 4.

$$\frac{[\text{Zn}]}{[\text{Zn}]_0} = 1 - \left(\delta^{66/64}\text{Zn} / 10^3 + 1 \right)^{1/\alpha-1} \quad (2)$$

with $[Zn]_0$ being the Zn concentration before the evaporation and α the kinetic fractionation factor that we approximated by $\sqrt{M^{64}Zn/M^{66}Zn}$ where $M^{64}Zn$ and $M^{66}Zn$ are the masses of ^{64}Zn and ^{66}Zn .

It can be seen from Fig. 4 that a Rayleigh distillation (black curve) does not account for the observed isotopic composition (black dots). A much larger isotopic fractionation would result from a simple Rayleigh distillation.

The slight enrichment in heavy isotopes of Zn of the rim in comparison to the core ($\delta^{66/64}Zn=1.83$ vs 1.22) of the flanged australite USNM 5772 may also be an argument in favor of vapor fractionation. If we consider that the evaporation follows a Rayleigh distillation law and using the difference of Zn contents between the rim (19 ppm) and the core (265 ppm), the isotopic effect between the rim and the core of the tektite gives $\delta^{66/64}Zn_{rim}-\delta^{66/64}Zn_{core}$ of ~41 ‰. This isotopic fractionation is much larger than the observations (~0.6 ‰), and, therefore, a simple Rayleigh distillation does not account for the mechanism of fractionation between the rim and the core of the australite flanged tektites.

A Rayleigh distillation assumes that the tektites are always homogeneous and that the evaporated Zn is always removed from the system. If we consider a tektite as a sphere, the Zn has to be removed from the surface and so induced chemical heterogeneities in the tektites. In the following part of the discussion, we describe a dynamic model of isotopic fractionation by evaporation at the surface of a molten sphere, the sphere being re-homogenized by diffusion and advection.

4. 3. Evaporation of Zn from a molten sphere

4.3.1 Description of the model

During its hypervelocity trajectory, the molten surface of the tektite will interact by viscous coupling with air, which will then induce a velocity field inside the molten sphere. This velocity field induces significant radial chemical mixing within the tektite, which speeds up the evaporation process. In order to model this effect, we use a velocity field calculated from the Rybczynski-Hadamard formulae (Grasset and Albarede, 1994; Levich, 1962), which is a solution of the Navier-Stokes equation for the steady motion of a viscous sphere within a viscous media.

$$\begin{cases} v_{\theta}(r, \theta) = U_0 \left[2 \left(\frac{r}{R_{Tec}} \right)^2 - 1 \right] \sin \theta \\ v_r(r, \theta) = U_0 \left[1 - \left(\frac{r}{R_{Tec}} \right)^2 \right] \cos \theta \end{cases} \quad (\text{eq. 3})$$

The velocity field obtained using the Rybczynski-Hadamard formula only involves one free parameter U_0 , which we call the surface velocity. We numerically solved the transport equation in spherical coordinate using an explicit finite different method with a first order upwind approximation for the advective term (Forsythe and Wasow, 1960)

$$\frac{\partial C(r, \theta, t)}{\partial t} = \frac{1}{Pe} \Delta C(r, \theta, t) - \vec{v}(r, \theta) \cdot \vec{\nabla} C(r, \theta, t) \quad (\text{eq. 4})$$

The Peclet number is defined as $Pe=U_0R_{Tec}/D_{Zn}$ where R_{Tec} is the tektite radii and D_{Zn} is the diffusivity of zinc within the silicate melt. Equation 2 is solved independently for ^{68}Zn and ^{64}Zn

assuming they have the same diffusivity D_{Zn} . Because the diffusivity of Zn in silicate liquid has never been measured, we chose a value of $10^{-8} \text{ m}^2/\text{s}$, because this value is a likely upper limit for diffusion coefficient of a cation within a silicate liquid (Brady, 1995). However, as shown by Jourdan et al. (2007) for the diffusion of noble gas in tektite, the diffusion coefficient, i.e. the speed at which a given elements diffuse within the grain is strongly dependent on the polymerization level of the target rock. In other words, the more the target rock is rich in silica, the more the diffusion of a given elements will be slow.

Calculations are run using a 40 x 40 grid (in theta and r space). Boundary conditions express continuity along the symmetry axis, while at the surface we set an evaporation flux:

$$\begin{cases} J_t^{68} = -\left[{}^{68}\text{Zn} \right]_r / \tau_{evap} \\ J_t^{64} = -\sqrt{\frac{68}{64}} \left[{}^{64}\text{Zn} \right]_r / \tau_{evap} \end{cases} \quad (\text{eq. 5})$$

τ_{evap} is a model input parameter which controls how fast evaporation takes place at the outer boundary. A high value of τ_{evap} corresponds to a slow evaporation, whereas low values of τ_{evap} imply fast evaporation. Calculations are extended up to $t_{\text{max}}=5$ s, which is of the order of the tektite ballistic trajectory duration.

4.3.2 Results and discussion of the model

For a given radii there are three timescales that will control the magnitude of Zn evaporation and isotopic fractionation: i) the evaporation timescale τ_{evap} ii) the advection timescale $\tau_{adv} = R_{\text{Tec}}/U_0$ which controls how fast mixing occurs inside the sphere iii) the diffusion timescale τ_{diff} which we express as $\tau_{diff} = \frac{L^2}{D_{Zn}}$, where L is the thickness of the boundary layer.

These three timescales have competing effects on the magnitude of the isotopic fractionation. If the advection and diffusion timescale are short with regard to the evaporation timescale, the sphere will be well mixed during the evaporation process and the system will evolve with Rayleigh distillation behavior. However if τ_{adv} or τ_{diff} are long with regard to the evaporation timescale, the system deviates from a Rayleigh behaviour.

This effect can be observed on figure 5. In this figure, the evolution of the ${}^{68}\text{Zn}$ concentration is shown while evaporation progresses, for different values of τ_{evap} . For low values of τ_{evap} (0.1 and 1 s) a kink appears in the evaporation curves, which corresponds to the apparitions of the diffusion limited regime.

The apparition of the diffusion limited regime has a strong impact on the isotopic evolution of the tektite. Figure 6 shows the bulk isotopic composition of the tektite for different values of the evaporation timescale. For $\tau_{evap} > 1$ s the bulk isotopic fractionation increases as τ_{evap} decreases (evaporation is faster and the tektite loses more Zn over the 5 s duration of the calculations). This is the expected behaviour for Rayleigh fractionation, which leads to strong isotopic fractionation (Fig. 4 and 6). Oppositely, for $\tau_{evap} < 1$ s the isotopic fractionation strongly decreases together with τ_{evap} decrease. In this diffusion limited regime, strong Zn losses are obtained with minor isotopic fractionation. This regime explains well the small isotopic

fractionation we measured in tektites (up to a few permil for the $^{68}\text{Zn}/^{64}\text{Zn}$ ratio), even though the tektite appears to have experienced large evaporation (~60 % Zn loss).

The effect of surface velocity was investigated (Fig. 7). As expected, for large values of the surface velocity ($V_0 > 10^{-2}$ m/s) the bulk isotopic composition evolves as Rayleigh fractionation (i.e., well mixed). For lower values the system deviates from this behavior, and isotopic fractionations obtained are lower than in the case of the Rayleigh distillation (Fig. 7). This effect can be understood if one considers the chemical boundary layer at the surface of the

molten sphere, which is of the order $L = \left(\frac{R_{rec} D_{Zn}}{V_0} \right)^{\frac{1}{2}}$ (Levich, 1962). By decreasing the surface velocity, the boundary layer thickens and the diffusion timescale increases.

Because the measurements in tektites show moderate isotopic fractionation with regard to a Rayleigh model, we suggest that evaporation took place in a diffusion-limited regime. This is corroborated by the observation that rims and cores of an australite sample do not have large isotopic variation. From our model, such a regime is obtained for values of the surface velocity below 1 cm/s. As the value we used for the Zn diffusion coefficient is likely an upper limit (10^{-8} m²/s), the value of V_0 is also an upper limit. We note that we assumed a non-ideal behaviour for the isotopic effect on Zn diffusion (i.e., $D_{Zn}^{64} = D_{Zn}^{68}$). Although there is no experimental evidence against or in favor of this hypothesis, differential diffusion of Zn isotopes would produce an additional source of isotopic fractionation (Richter, 2004).

Finally, we note that the lack of strong isotopic fractionation observed for potassium or boron (Chaussidon and Koeberl, 1995; Humayun and Koeberl, 2004) does not preclude evaporation. Similarly to what has been proposed here for Zn, if K and B evaporation took place in a diffusion-limited regime the isotopic fingerprint might be small (< 1 permil) even if significant amounts of K or B were lost.

5. Conclusions

In order to study the effects of the volatilization in tektites we measured the Zn isotopic composition of 20 tektites from the four different strewn fields. Almost all the tektites are enriched in heavy isotopes of Zn compared to the upper continental crust with a full range in $\delta^{66/64}\text{Zn}$ of about two permil. On average the different groups of tektites are isotopically distinct and give the following values (from the isotopically lightest to the heaviest): Muong-Nong type indochinites ($\delta^{66/64}\text{Zn} = 0.61 \pm 0.30$); the North American bediasites ($\delta^{66/64}\text{Zn} = 1.61 \pm 0.49$); the Ivory Coast tektites ($\delta^{66/64}\text{Zn} = 1.66 \pm 0.18$); the Australasian tektites (others than the Muong Nong-type indochinites) ($\delta^{66/64}\text{Zn} = 1.84 \pm 0.42$) and the Central European moldavites ($\delta^{66/64}\text{Zn} = 2.04 \pm 0.19$).

The negative correlation between $\delta^{66/64}\text{Zn}$ and the abundance of Zn, may reflect that the isotopic fractionation occurred by evaporation during the heating event of the tektites. A simple Rayleigh distillation model can not account for the observations. We developed a more realistic model of evaporation of Zn from a molten sphere: during its hypervelocity trajectory, the molten surface of the tektite will be entrained by viscous coupling with air, which will then induce a velocity field inside the molten sphere. This velocity field induces significant radial chemical mixing within the tektite which fastens the evaporation process. This model, even if parameter

dependent, shows that the isotopic composition measured in tektites can be produced by evaporation in a diffusion-limited regime.

Acknowledgments: CK was supported by the Austrian Science Foundation.

References:

- Albarede, F., 2004. The stable isotope geochemistry of copper and zinc. In: CM. Johnson, B.Beard, F.Albarede (Eds), *Geochemistry of Non-Traditional Stable Isotopes. Reviews In Mineralogy & Geochemistry*, Mineralogical Society of America, Geochemical Society. Vol. 55. pp.409-427.
- Albarede, F., Bunch, T.E., Moynier, F. and Douchet, C., 2007. Isotope fractionation during impact: Earth versus the moon (abstract). *Meteoritics & Planetary Science*, 42: A11-A11.
- Ben Othman, D., Luck, J.M., Bodinier, J.L., Arndt, N.T. and Albarede, F., 2006. Cu-Zn isotopic variations in the Earth's mantle (abstract). *Geochimica et Cosmochimica Acta* 70: A46.
- Blum, J.D., Papanastassiou, D.A., Wasserburg, G.J. and Koeberl, C., 1992. Neodymium and strontium isotopic study of Australasian tektites - New constraints on the provenance and age of target materials. *Geochimica et Cosmochimica Acta*, 56: 483-492.
- Brady, J.B., 1995. Diffusion data for silicate minerals, glasses and liquids. in: T. Ahrens (Ed), *Mineral physics and crystallography, a handbook of physical constants*, Am. Geophys. Union, Washington, D.C.
- Chaussidon, M. and Koeberl, C., 1995. Boron content and isotopic composition of tektites and impact glasses: Constraints on source regions. *Geochimica et Cosmochimica Acta*, 59: 613-624.
- Cloquet, C., Carignan, J. and Libourel, G., 2006. Isotopic composition of Zn and Pb atmospheric depositions in an urban/periurban area of northeastern France. *Environmental Science & Technology*, 40: 6594-6600.
- Engelhardt, W.V., Luft, E., Arndt, J., Schock, H. and Weiskirchner, W., 1987. Origin of moldavites. *Geochimica et Cosmochimica Acta*, 51: 1425-1443.
- Esat, T. and Taylor, S., 1986. Mg isotope composition of Ivory Coast microtektites (abstract) *Lunar and Planetary Science* 17: 210-211.
- Esat, T., and Taylor, S.R., 1987. Mg isotopic composition of microtektites and flanged australite buttons. *Lunar and Planetary Science* 18: 267-268.
- Forsythe, G.E. and Wasow, R., 1960. *Finite-difference methods for partial differential equations*. Wiley & Sons, New York, 444 p.
- Glass, B.P., 1990. Tektites and microtektites: key facts and inferences. *Tectonophysics*, 171: 393-404.
- Glass, B. and Koeberl, C., 1989. Trace elements of high and low refractive index Muong Nong type tektites from Indochina. *Meteoritics*, 24: 143-146.
- Grasset, O. and Albarede, F., 1994. Hybridization of mingling magmas with different densities. *Earth and Planetary Science Letters*, 121: 327-332.

- Greenland, L.; Lovering, J. F., The evolution of tektites: elemental volatilization in tektites. *Geochimica et Cosmochimica Acta*, 27:249-259
- Herzog, G.F., Alexander, C.M. O'D., Glass, B.P., Berger, E.L., and Delaney, J.S., 2005. Potassium isotope fractionation in Australasian microtektites: Evidence for evaporation and re-condensation in a vapor plume. *Lunar and Planetary Science* 36, abstract No. 1167 (CD-ROM).
- Humayun, M. and Clayton, R.N., 1995. Potassium isotope cosmochemistry: Genetic implications of volatile element depletion. *Geochimica et Cosmochimica Acta*, 59: 2131-2148.
- Humayun, M. and Koeberl, C., 2004. Potassium isotopic composition of Australian tektites. *Meteoritics and Planetary Science*, 39: 1509-1516.
- John, S. G., Geis, R., Saito, M., and Boyle, E. A., 2007. Zn isotope fractionation during high-affinity zinc transport by the marine diatom *Thalassiosira oceanica*. *Limnol. Oceanogr.* 52, 2710-2714.
- Jourdan, F., Renne, P.R., Reimold, U.W., 2007. The problem of inherited $^{40}\text{Ar}^*$ in dating impact glass by $^{40}\text{Ar}/^{39}\text{Ar}$ geochronology: Evidence from the Tswaing crater (South Africa). *Geochim. Cosmochim. Acta* 71, 1214-1231.
- Karikari, F., Ferrière, F., Koeberl, C., Reimold, W.U. and Mader, D., 2007. Petrography, geochemistry, and alteration of country rocks from the Bosumtwi impact structure, Ghana. *Meteoritics and Planetary Science*, 42: 513-540.
- Koeberl, C., 1985. Trace element chemistry of Libyan Desert Glass (abstract). *Meteoritics*, 20: 686.
- Koeberl, C., 1986. Geochemistry of tektites and impact glasses. *Annual Review of Earth and Planetary Sciences*, 14: 323-350.
- Koeberl, C., 1990. The geochemistry of tektites: an overview. *Tectonophysics*, 171: 405-422.
- Koeberl, C., 1992. Geochemistry and origin of Muong Nong-type tektites. *Geochimica et Cosmochimica Acta*, 56: 1033-1064.
- Koeberl, C., 1994. Tektite origin by hypervelocity asteroidal or cometary impact: Target rocks, source craters, and mechanisms. In: B.O. Dressler, R.A.F. Grieve, and V.L. Sharpton (Eds), *Large Meteorite Impacts and Planetary Evolution*, Geological Society of America Special Paper 293, 133-152.
- Koeberl, C., 2007. The geochemistry and cosmochemistry of impacts. In: A.Davis (Eds), *Treatise of Geochemistry*, online edition, Vol. 1,, Elsevier, p. 1.28.1 -1.28.52, doi:10.1016/B978-008043751-4/00228-5.
- Koeberl, C. and Shirey, S.B., 1993. Detection of a meteoritic component in Ivory Coast tektites with rhenium-osmium isotopes. *Science*, 261: 595-598.
- Koeberl, C., Poag, C.W., Reimold, W.U. and Brandt, D., 1996. Impact origin of the Chesapeake Bay structure and the source of the North American tektites. *Science*, 271: 1263-1266.
- Koeberl, C., Bottomley, R., Glass, B. and Storzer, D., 1997. Geochemistry and age of Ivory Coast tektites and microtektites. *Geochimica et Cosmochimica Acta*, 61: 1745-1772.
- Koeberl, C., Reimold, W.U., Blum, J. and Chamberlain, C., 1998. Petrology and geochemistry of target rocks from the Bosumtwi impact structure, Ghana, and comparison with Ivory Coast tektites. *Geochimica et Cosmochimica Acta*, 62: 2179-2196.
- Levich, V.G., 1962. *Physicochemical Hydrodynamics*. Prentice-Hall, Englewood Cliffs, 700 pp.
- Lodders, K., 2003. Solar system abundances and condensation temperatures of the elements. *Astrophysical Journal*, 591: 1220-1247.

- Ma P., Aggrey K., Tonzola C., Schnabel C., de Nicola P., Herzog G., T., Wasson J. T., Glass B. P., Brown L., Tera F., Middleton R., and Klein J., 2004. Beryllium-10 in Australasian tektites: constraints on the location of the source crater. *Geochimica et Cosmochimica Acta* 68: 3883–3896.
- Maréchal, C. Telouk, P. and Albarede, F., Precise analysis of copper and zinc isotopic compositions by plasma-source mass spectrometry, *Chemical Geology* 156 (1999) 251-273.
- Maréchal, C.N., Douchet, C., Nicolas, E. and Albarède, F., 2000. The abundance of zinc isotopes as a marine biogeochemical tracer. *Geochemistry, Geophysics, Geosystems* 1: 1999GC-000029.
- Moynier, F., Albarede, F. and Herzog, G., 2006. Isotopic composition of zinc, copper, and iron in lunar samples. *Geochimica et Cosmochimica Acta*, 70: 6103-6117
- Moynier, F., Blichert-Toft, J., Telouk, P., Luck, J.M. and Albarede, F., 2007. Comparative stable isotope geochemistry of Ni, Cu, Zn, and Fe in chondrites and iron meteorites. *Geochimica et Cosmochimica Acta*, 71: 4365-4379.
- Moynier, F., Pichat, S., Pons, M.-L., Fike, D., Balter, V., and Albarede, F., In press. Isotopic fractionation and transport mechanisms of Zn in plants. *Chemical Geology*.
- Pichat, S., Douchet, C., Albarède, F., 2003. Zinc isotope variations in deep-sea carbonates from the eastern Equatorial Pacific over the last 175 ka. *Earth and Planetary Science Letters* 210 (1–2), 167–178.
- Richter, F.M., 2004. Timescales determining the degree of kinetic isotope fractionation by evaporation and condensation. *Geochimica et Cosmochimica Acta*, 68: 4971-4992.
- Rudnick, R.L. and Gao, S., 2003. Composition of the Continental Crust. In: H.D. Holland and K.K. Turekian (Editors), *Treatise on Geochemistry*, pp. 1-64. Elsevier. Amsterdam.
- Serefiddin, F., Herzog, G.F., and Koeberl, C., 2007. Beryllium-10 concentrations of tektites from the Ivory Coast and from Central Europe: Evidence for near-surface residence of precursor materials. *Geochimica et Cosmochimica Acta* 71: 1574-1582.
- Taylor, S.R., 1961, Distillation of alkali elements during formation of australite flanges, *Nature*, 189, 630-633
- Taylor, H.P. and Epstein, S., 1962, Oxygen isotopic study on the origin of tektites, *Journal of Geophysical Research*, 67, 4485-4490.
- Taylor, H.P. and Epstein, S., 1964, Comparison of oxygen isotope analyses of tektites, soils and impact glasses. In: H. Craig, L. Miller, G.J. Wasserburg, (Eds) *Isotopic and Cosmic Chemistry*, North Holland Amsterdam. 181-199.
- Viers, J., Oliva, P., Nonelle, A., Gelabert, A., Sonke, J., Freydier, R., Gainville, G., Dupre, B., 2007 Evidence of Zn isotopic fractionation in a soil-plant system of a pristine tropical watershed (Nsimi, Cameroon), *Chemical Geology* 239 124-137
- Walter, L.S., 1967. Tektite compositional trends and experimental vapor fractionation of silicates. *Geochimica et Cosmochimica Acta*, 31: 2043-2063.
- Walter, L.S., and Clayton, R.N., 1967. Oxygen isotopes: Experimental vapor fractionation and variations in tektites. *Science* 156, 1357-1358.
- Weinke, H.H. and Koeberl, C., 1985. Trace elements in two bediasite tektites (abstract). *Meteoritics*, 20: 783.
- Weiss, D. J., Mason, T. F. D., Zhao, F. J., Kirk, G. J. D., Coles, B. J., and Horstwood, M. S. A., 2005. Isotopic discrimination of zinc in higher plants. *New Phytologist* **165**, 703-710.

Figure Captions:

Fig. 1: $\delta^{68}\text{Zn}$ vs $\delta^{66}\text{Zn}$. All the samples (but 2) fall on the mass-dependent fractionation line of slope 1.94. The two samples outside the mass-dependent fractionation line have been excluded of the discussion.

Fig. 2: $\delta^{66}\text{Zn}$ vs $[\text{Zn}]$ for all the tektites analyzed in this study. This (weak) negative correlation may reflect that the isotopic fractionation occurred during evaporation of Zn ($[\text{Zn}]$ decreases and $\delta^{66}\text{Zn}$ increases because of the preferential loss of light isotopes in the vapor phase).

Fig. 3: $\delta^{66}\text{Zn}$ vs $[\text{Zn}]$ for the Australasian tektites.

Fig. 4: ^{66}Zn vs $[\text{Zn}]$ for all the tektites analyzed in this study. The black curve represents the evolution of the isotopic composition in the case of a Rayleigh distillation. A much larger isotopic fractionation than the observations would result from a Rayleigh distillation.

Fig. 5: Model calculations of the evaporation/mixing of Zn from a 1 mm radii molten sphere. Calculations are run with $U_0=4 \cdot 10^{-3}$ m/s and $D_{\text{Zn}}=10^{-8}$ m²/s. see text for discussion about the parameters.

Fig. 6: Bulk Zn isotopic composition of the tektite as a function of the evaporation timescale.

Fig. 7: Bulk isotopic composition as a function of the amount of residual Zn, for different values of the surface velocity. Calculations were run for $t_{\text{max}}=5\text{s}$, $D_{\text{Zn}}=1\text{e}^{-8}$ m²/s, $R=1$ mm and $\tau_{\text{evap}}=2\text{s}$.

Table 1: Isotopic composition and concentration of Zn in tektites. The isotopic composition is represented using the δ notation (per 1000) and the concentrations are in ppm.

Sample name	$\delta^{66}\text{Zn}$	$\delta^{68}\text{Zn}$	[Zn] ppm
Ivory Coast 8902	1.62	3.20	24 ^a
Ivory Coast 3395	1.51	3.09	3 ^a
Ivory Coast 2014	1.86	3.81	2 ^a
Bediasite 8402	1.46	3.43	26
Bediasite 8401	1.78	4.13	11
Moldavite Jankov 1	1.92	4.34	29
Moldavite Jankov 2	1.93	4.16	23
Moldavite Jankov 4	2.22	4.82	24
Moldavite Chlum	2.27	4.63	19
Hainan HSF1	2.16	4.47	7.8
Muong Nong 8301	0.31	0.82	90 ^b
Muong Nong 8309	0.61	1.32	74 ^b
Muong Nong 8314	0.71	1.40	65 ^b
Muong Nong X102	0.90	1.95	20 ^c
Muong Nong X103	0.51	1.16	69 ^c
Philippinite 1995	2.49	4.98	19
Philippinite P9201	1.48	3.30	23
Thailandite 8204	1.75	3.51	7.6
Australite 5772 Core	1.22	3.47	265
Australite 5772 Rim	1.83	3.82	19
Australite T8205	1.96	4.23	16
Lybian Desert Glass LDG8501	0.61	1.21	121

^a(Koeberl et al., 1997)

^b(Koeberl, 1992)

^c(Glass and Koeberl, 1989)

Table 2: Trace element composition of the different tektites analyzed for their Zn isotopic compositions. All the elemental abundances at the exception of Ba, Cr and Ni have been analyzed by ICP-MS. Ba, Cr and Ni abundances have been measured by ICP-AES. Data listed in ppm ($\mu\text{g/g}$). - : below detection limit.

Sample name	Li	Be	Ti	V	Cr	Mn	Co	Ni	Cu	Zn	As	Se	Rb	Sr	Y	Sn	Sb	Ba	La	Ce	Pr	Nd	Sm	Eu	Gd	Tb	Dy	Ho	Er	Yb	Pb	U
Bediasite 8402	19	1.2	3975	68	18	365	11	3	6.5	26	0.5	3.6	77	169	12	0.7	0.3	462	8.9	22	3.6	13	3.0	-	1.8	-	1.5	0.0	0.4	0.5	8.0	6.4
Bediasite 8401	16	1.7	3310	49	13	322	10	-	3.8	11	0.8	2.9	71	197	12	0.3	0.2	471	10	22	3.7	14	3.0	0.3	2.2	-	1.9	0.2	0.9	0.8	15	3.9
Moldavite Jankov 1	53	1.7	2196	36	32	556	6	-	-	29	0.7	3.6	159	157	9.0	0.8	0.3	801	9.7	20	3.3	12	2.6	0.0	1.6	-	1.2	0.0	0.4	0.4	7.3	7.0
Moldavite Jankov 2	49	1.7	2152	32	25	843	6	4	0.1	23	0.5	2.8	139	167	9.3	0.7	0.2	798	9.9	20	3.4	13	2.6	0.1	1.7	-	1.3	0.1	0.5	0.5	6.0	8.1
Moldavite Jankov 4	54	1.6	2092	34	-	577	6	-	0.1	24	0.5	3.6	158	159	8.9	0.6	0.2	-	9.4	19	3.2	12	2.6	0.0	1.5	-	1.1	0.0	0.4	0.4	5.9	8.3
Moldavite Clum	43	1.5	2087	26	9	928	5	-	-	19	0.4	3.1	122	158	9.5	0.5	0.2	604	9.4	21	3.5	12	2.6	-	1.6	-	1.1	-	0.2	0.3	3.6	7.1
Hainan HFS1	48	1.9	5117	79	32	733	12	-	2.2	7.8	1.0	3.9	119	145	16	0.4	0.3	336	14	30	4.8	17	3.6	0.1	2.6	-	2.3	0.2	1.1	1.1	1.6	7.1
Philippinite 1995	55	2.1	5432	99	72	883	16	31	3.8	19	1.3	2.6	130	187	16	1.1	0.4	346	15	30	4.9	18	3.7	0.2	2.8	-	2.4	0.3	1.2	1.1	6.6	9.5
Philippinite P9201	47	1.7	4558	83	49	853	13	17	2.2	23	1.5	2.9	114	220	14	1.2	0.5	320	13	26	4.3	16	3.4	0.1	2.3	-	2.1	0.2	0.9	0.9	7.7	7.4
Thailandite 8204	49	2.0	5351	77	37	782	11	5	0.8	7.6	1.0	4.5	113	157	15	0.7	0.4	347	15	29	4.7	18	3.7	0.1	2.5	-	2.2	0.2	0.9	1.0	2.7	5.4
Australite 5772 Core	48	1.9	4890	94	31	816	14	6	4.5	265	1.9	3.6	116	246	15	1.0	0.4	401	14	28	4.6	17	3.5	0.1	2.6	-	2.3	0.2	1.0	1.0	5.5	9.5
Australite 5772 Rim	44	0.8	5039	72	35	824	12	10	0.9	19	0.1	7.2	108	232	14	0.8	0.7	335	14	28	4.3	18	4.1	-	1.4	-	1.1	-	-	-	2.6	5.7
Australite T8205	56	1.8	5453	90	34	842	15	23	1.8	16	0.8	4.0	117	222	16	1.0	0.5	356	15	31	5.0	19	4.0	-	2.4	-	2.1	0.1	0.8	0.9	5.3	6.1
Lybian Desert Glass LDG8501	4.6	0.4	1083	5.3	-	14	0.3	-	1.3	4.2	0.1	0.1	0.4	20	2.2	0.2	-	19	3.6	7.5	1.1	3.5	0.6	0.3	0.7	0.1	0.4	0.0	0.2	0.2	6.9	2.6

Table 3: Some major element composition of the tektites analyzed for their Zn isotopic compositions. Data reported in wt%,

Sample name	Na	Mg	Al	K	Ca	Fe
Bediasite 8402	1.04	0.37	4.44	1.63	0.47	2.22
Bediasite 8401	0.97	0.28	4.32	1.60	0.41	1.89
Moldavite Jankov 1	0.35	1.17	5.54	3.01	1.78	1.34
Moldavite Jankov 2	0.31	1.52	5.20	2.85	2.29	1.30
Moldavite Clum	0.20	1.49	3.84	2.39	2.45	1.17
Hainan HFS1	0.82	0.93	4.41	1.79	1.15	2.81
Philippinite 1995	0.80	1.24	5.50	1.63	1.56	3.15
Philippinite P9201	0.66	1.12	4.96	1.49	2.23	2.75
Thailandite 8204	0.63	1.02	5.15	1.44	1.19	2.72
Australite 5772 Core	0.72	0.98	4.05	1.58	2.10	2.83
Australite 5772 Rim	0.51	1.01	4.91	1.33	1.93	2.67
Australite T8205	0.63	1.25	4.57	1.55	2.16	3.10
Lybian Desert Glass LDG8501	-	0.02	0.55	0.01	0.02	0.09

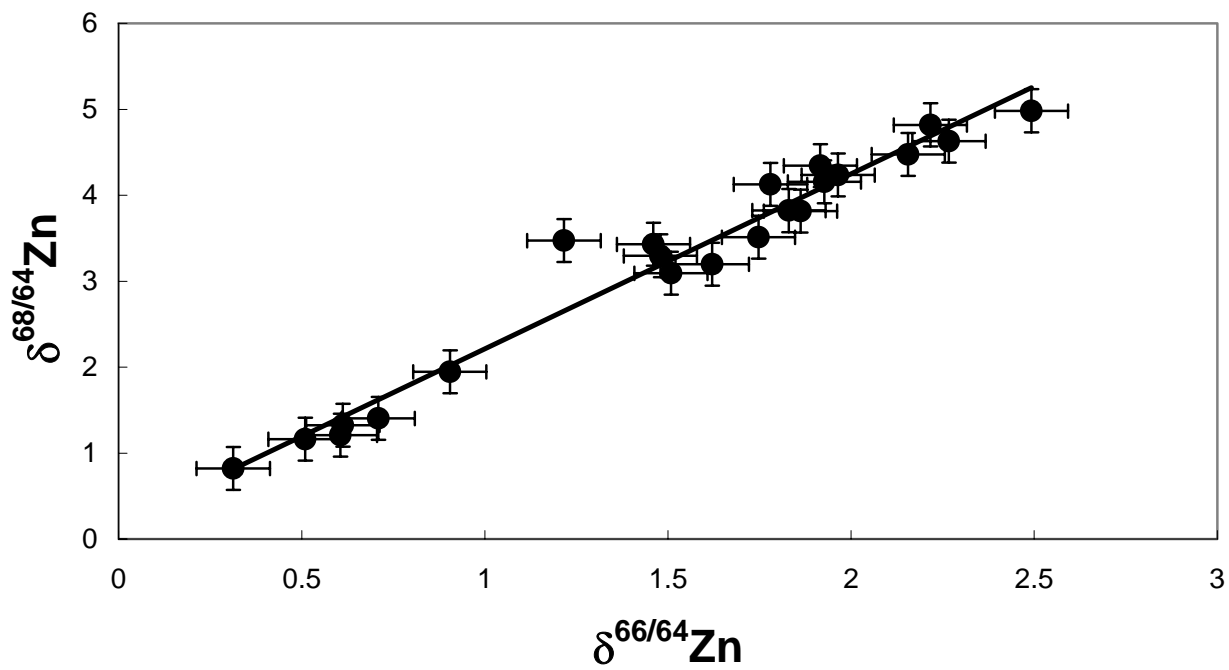


Figure 1

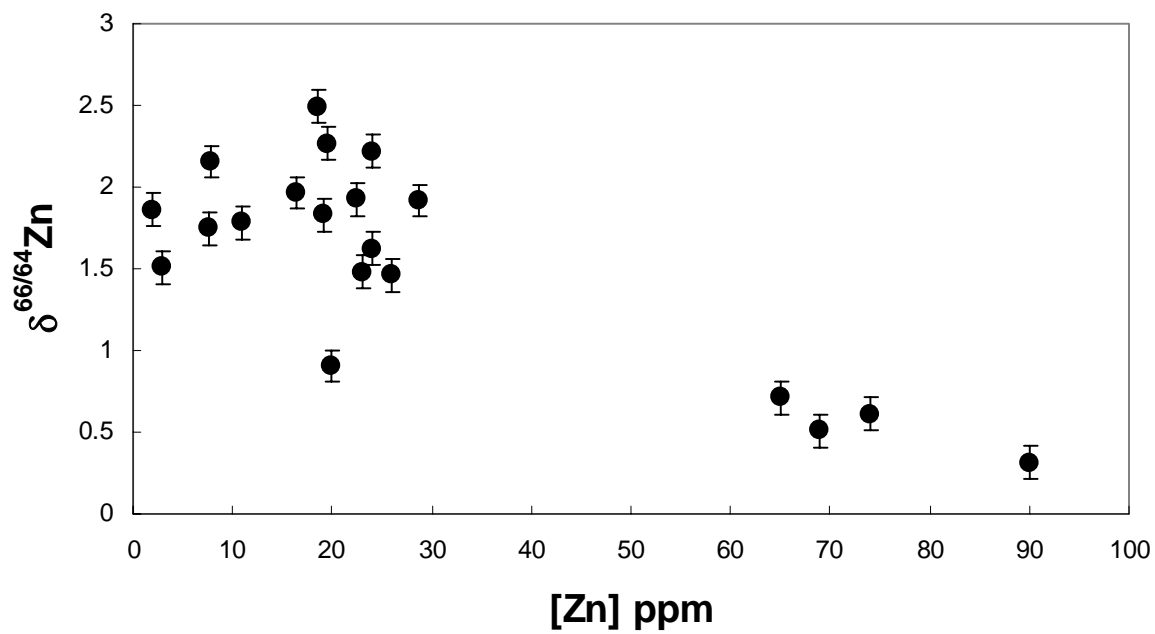


Figure 2

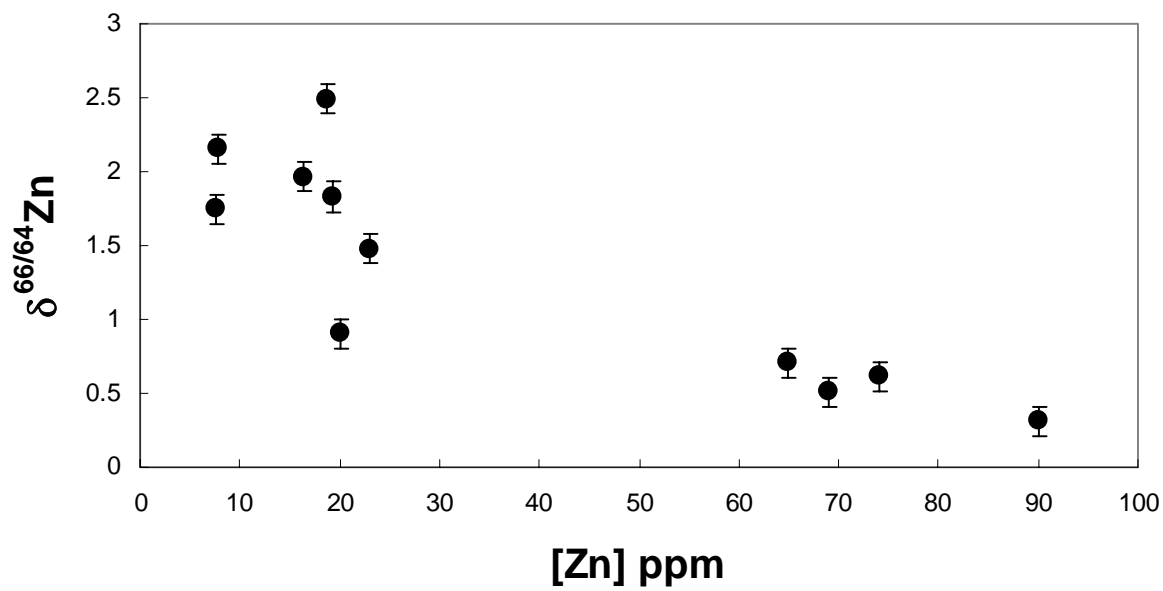


Figure 3

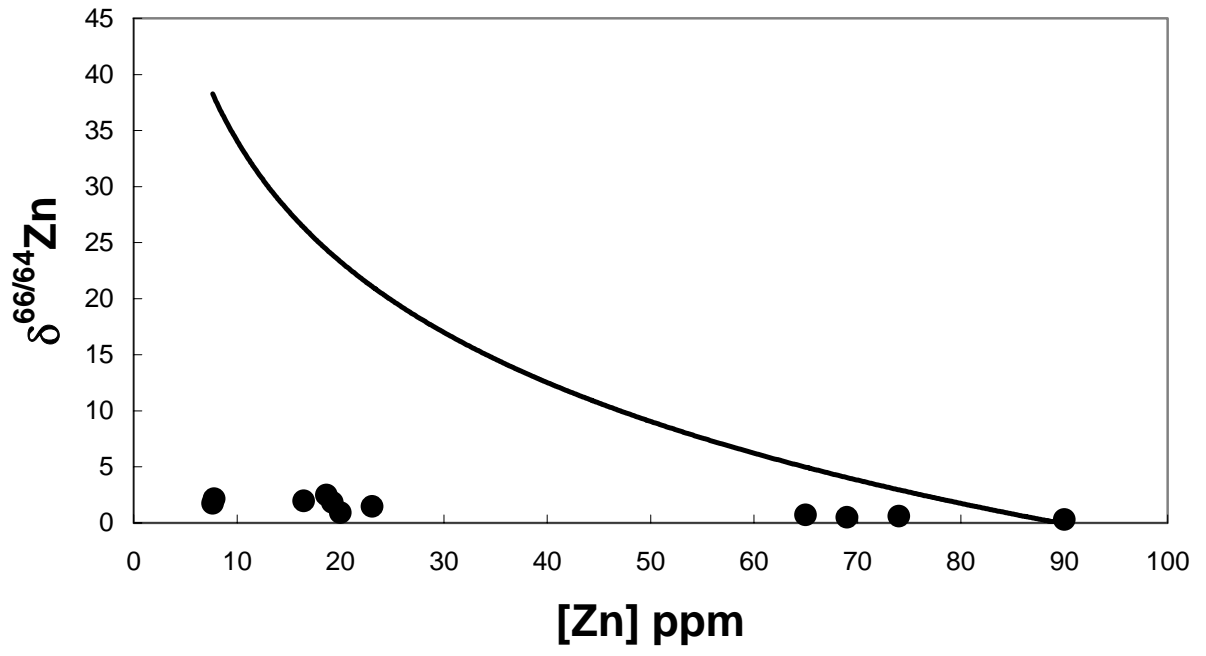


Figure 4

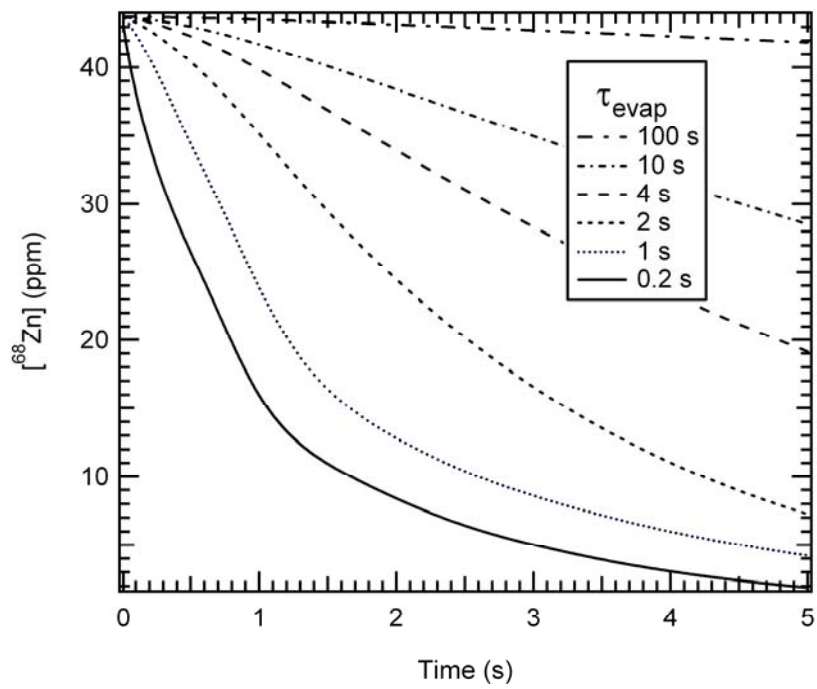


Figure 5:

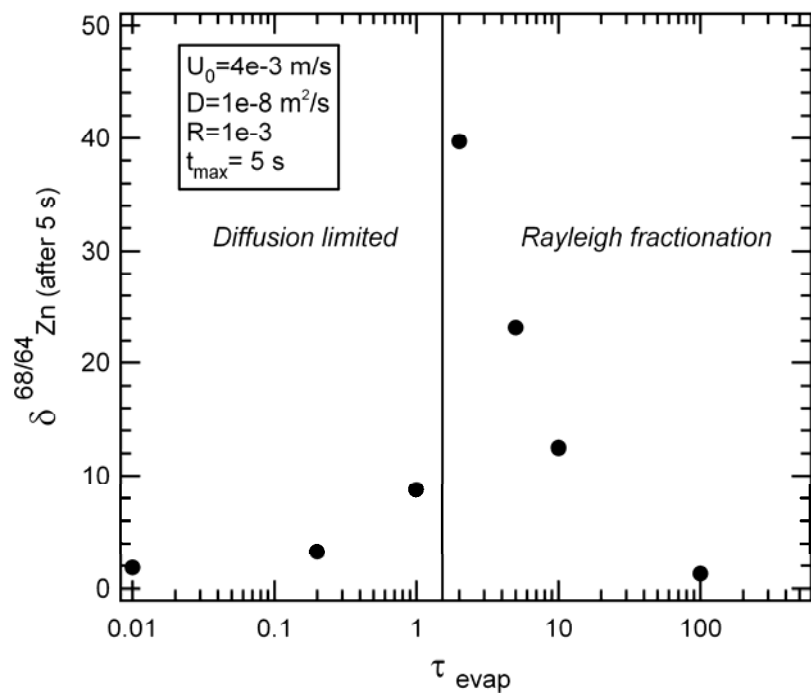


Figure 6:

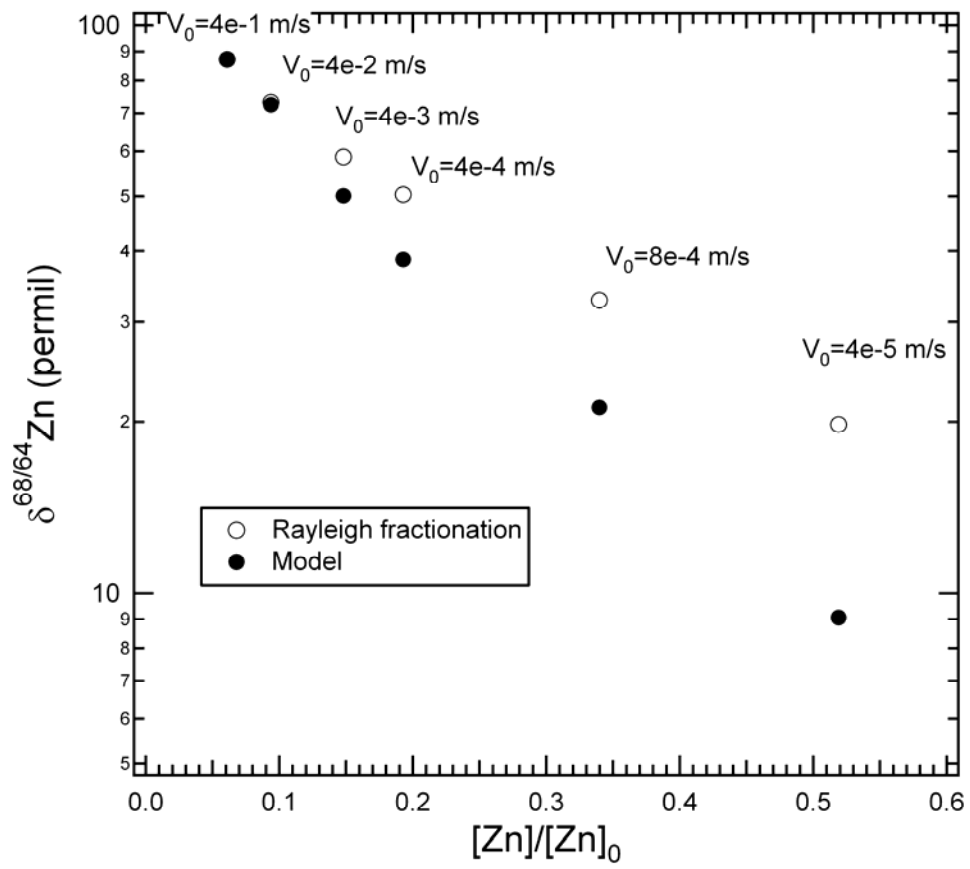


Figure 7: